

Electrical and thermal transport properties of magnetically aligned single wall carbon nanotube films

J. Hone, M. C. Llaguno, N. M. Nemes, and A. T. Johnson

Department of Physics and Laboratory for the Research on the Structure of Matter, University of Pennsylvania, Philadelphia, Pennsylvania 19104

J. E. Fischer^{a)}

Department of Materials Science and Engineering and Laboratory for the Research on the Structure of Matter, University of Pennsylvania, Philadelphia, Pennsylvania 19104

D. A. Walters, M. J. Casavant, J. Schmidt, and R. E. Smalley

Center for Nanoscale Science and Technology, Rice University, Houston, Texas 77259

(Received 21 April 2000; accepted for publication 5 June 2000)

Dense, thick films of aligned single wall carbon nanotubes and nanotube ropes have been produced by filtration/deposition from suspension in strong magnetic fields. Electrical resistivity exhibits moderate anisotropy with respect to the alignment axis, while the thermopower is the same when measured parallel or perpendicular to this axis. Both parameters have identical temperature dependencies in the two orientations. Thermal conductivity in the parallel direction exceeds 200 W/mK, within a decade of graphite. © 2000 American Institute of Physics.

[S0003-6951(00)05231-1]

Bulk samples of parallel single-walled nanotubes (SWNTs) would constitute a fascinating new material, with highly anisotropic electrical and thermal transport properties. In this letter we report quantitative measurements of the anisotropic electrical and thermal transport properties of aligned thin films of SWNT ropes deposited from suspension in a high magnetic field.¹ The aligned samples show high electrical (σ) and thermal (κ) conductivity parallel to the H -alignment axis, while σ is significantly lower in the perpendicular direction. The thermoelectric power is independent of orientation.

The structural anisotropy of the two samples studied is described in the previous letter.² The “thin” and “thick” samples had effective thicknesses of $\sim 1.3 \mu\text{m}$ and $\sim 5 \mu\text{m}$, respectively, where we define t_{eff} as the measured mass per unit area divided by 1.33 g/cm^3 , the ideal density of close-packed tubes of average radius 1.4 nm. Using the same approach, the effective density was the highest yet observed on any bulk SWNT material; about half the crystallographic value. The SWNT ropes were aligned in the magnetic field direction, with a mosaic spread of 28° in the thin sample and 35° in the thick sample. Our measurements in the as-deposited, or unannealed state, were performed with the films still on their nylon filter membranes. Another series was measured after peeling the film off the filter and vacuum annealing at 1200°C , a process which is known to remove acid and surfactant residues from the purification and filtration, and to improve the crystallinity.³ The films peel away from the filter in the form of long narrow strips parallel to the field direction, a consequence of rope alignment. We therefore measured multiple samples to make sure that incipient tearing along the H direction did not affect the transverse properties and thus overestimate the anisotropy.

Figure 1 shows the temperature dependence of the normalized resistance R for the thick material, measured in both orientations on two different samples using a standard four-probe in-line technique. Before annealing, R shows a metallic temperature dependence above 150 K and nonmetallic behavior below, consistent with previous results on random as-grown⁴ and purified material.³ After annealing $R(T)$ is nonmetallic over the entire range, again consistent with previous results on unoriented material.³ Although the longitudinal and transverse conductance of a single crystalline rope should exhibit different temperature dependencies, we observe that the normalized $R(T)$ s are essentially identical in both directions, both before and after annealing. Since the

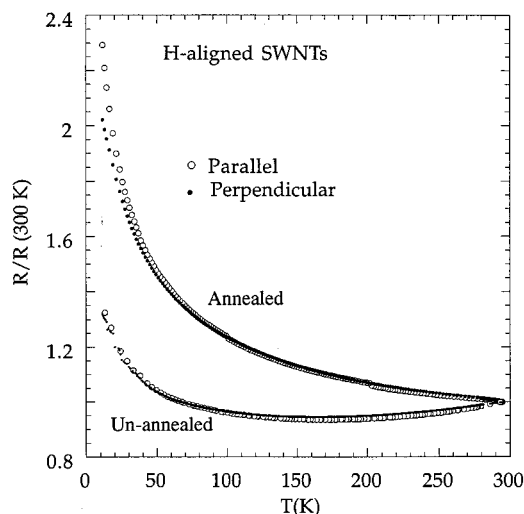


FIG. 1. Resistance vs temperature, normalized to 300 K, for the thick aligned SWNT sample before and after annealing. The unannealed sample is weakly metallic above ~ 150 K while the T dependence after annealing is nonmetallic over the entire range. In both cases R_{\parallel} and R_{\perp} display identical temperature dependencies.

^{a)}Electronic mail: fischer@sol1.lrsm.upenn.edu

TABLE I. Room-temperature resistivities of aligned SWNT samples (based on an effective thickness to account for porosity). In the parallel direction, the resistivity is close to that of Individual SWNT ropes.

Sample	ρ_{\parallel} (m Ω cm)	ρ_{\perp} (m Ω cm)	$\rho_{\perp} / \rho_{\parallel}$
Thin unannealed	0.095	2.3	24
Thin annealed	0.72
Thick unannealed	0.125	0.770	6
Thick annealed	0.825	5.0	6

alignment is not perfect,² it is likely that current flow is primarily along ropes in both directions, following a tortuous path in the perpendicular direction.

Table I shows $\rho = 1/\sigma$ at 300 K, for four representative samples, calculated using t_{eff} . In all cases ρ is higher in the perpendicular direction than in the parallel direction, reflecting the structural anisotropy. For the thin sample, the anisotropy is ~ 24 , while the ratio is ~ 6 for the thick sample, consistent with a larger mosaic spread in the latter.² Annealing does not improve the anisotropy of the thick sample, while x-ray diffraction reveals a large improvement in crystallinity.² This suggests that large scale movement, as would be required to reorient or straighten misaligned or bent/curved ropes, does not occur at 1200 °C while the smaller-scale motion required to crystallize imperfect ropes does occur at this temperature. Annealing also removes residual acid and surfactant, and ρ increases by a factor ~ 7 , consistent with earlier observations.³ This behavior is most likely due to electronic “doping” of the SWNTs by the acid. The resistivity of the annealed material is of the same order as that of individual SWNT ropes, which typically display a four-probe resistivity 100–200 $\mu\Omega$ cm.^{5,6} This provides further evidence that interrope contacts do not dominate the resistivity of bulk samples.⁶

Figure 2 shows $\kappa(T)$ for the thick sample measured in the parallel direction. Measurements from 10 to 300 K were

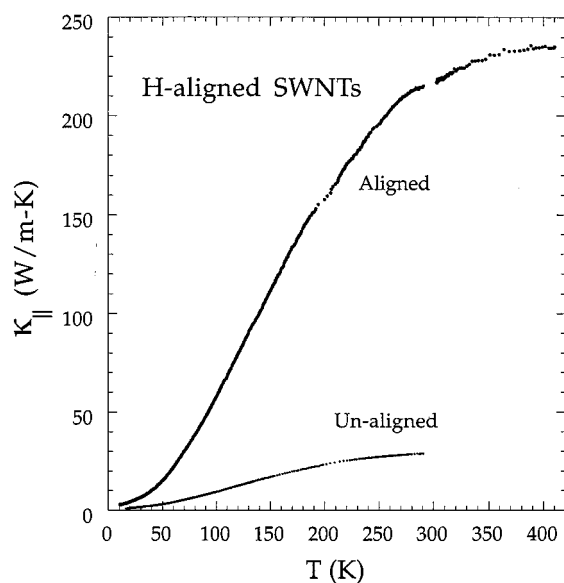


FIG. 2. Thermal conductivity of the “thick” annealed sample of aligned SWNT, measured in the parallel direction. At 300 K, κ is much higher than in unaligned material, and is within an order of magnitude of graphite (parallel to the layers) or diamond.

performed using a comparative technique. Heat was passed into the sample through a constantan rod, whose temperature-dependent thermal conductance was previously calibrated. The sample conductance was measured by comparing the temperature drop across the sample to that across the constantan, both of which were measured using 0.000 25 in. diameter thermocouple wires. At high temperatures, losses due to radiation can lead to an overestimate of κ ; a second constantan rod was used to measure the heat flow out of the sample to correct for these small losses. Above 300 K, a self-heating technique⁷ was used to measure κ of a sample small enough (< 1 mm) that the calculated losses due to radiation were insignificant. The thermal conductivity curves measured using both techniques match well at 300 K.

From 10 to 400 K, the thermal conductivity increases smoothly with increasing temperature, and displays a temperature dependence similar to that of unoriented SWNT.⁸ At room temperature, the thermal conductivity is greater than 200 W/m K, within an order of magnitude of that of diamond or graphite,⁹ and an order of magnitude greater than the previously reported thermal conductivity of unoriented material.⁸ Above 300 K, the thermal conductivity increases and then levels off near 400 K. Graphite and diamond, on the other hand, show a decreasing thermal conductivity with increasing temperature above ~ 150 K due to phonon-phonon Umklapp scattering. Extending this measurement to higher temperatures may provide insight as to whether the low dimensionality of nanotubes suppresses Umklapp processes, in which case better-aligned nanotubes could exhibit higher κ values at high T than graphite.

By measuring the thermal and electrical conductivities of a material, we can determine the electronic contribution to the thermal conductivity. In the measured sample, the ratio $\kappa/\sigma T$ has a value of $5 \times 10^{-6} \text{ V}^2/\text{K}^2$ at 300 K, essentially independent of temperature. This is more than two orders of magnitude greater than the value expected for electrons, indicating that κ is dominated by phonons, at least down to 10 K. We also note that $\kappa/\sigma T$ is identical in the oriented and unoriented material, even though their thermal conductivities differ by an order of magnitude. Therefore the anisotropy in the thermal conductivity (which we have not been able to measure reliably due to tears in the film) should follow the anisotropy in the electrical conductivity in aligned materials. Furthermore, it is likely that single ropes, which have a conductivity ~ 5 times that of σ_{\parallel} , will have a correspondingly larger thermal conductivity, and that individual tubes will have still higher thermal conductivities.

Figure 3 shows the measured thermoelectric power (TEP) of the thick sample. After annealing, the TEP is large and positive and increases with T , characteristic of a moderately p -doped semiconductor. This behavior is similar to that of as-grown SWNT.¹⁰ Recent reports¹¹ have shown that the positive TEP in SWNTs is a result of exposure to oxygen. Our samples were handled in air after the vacuum-annealing step, so the positive TEP is consistent with oxygen doping. The unannealed sample also shows a positive temperature-dependent TEP but smaller in magnitude. This is suggestive of a stronger hole-doping process by the acids used in purification,¹² which are removed by annealing. Both samples show virtually identical behavior in the parallel and

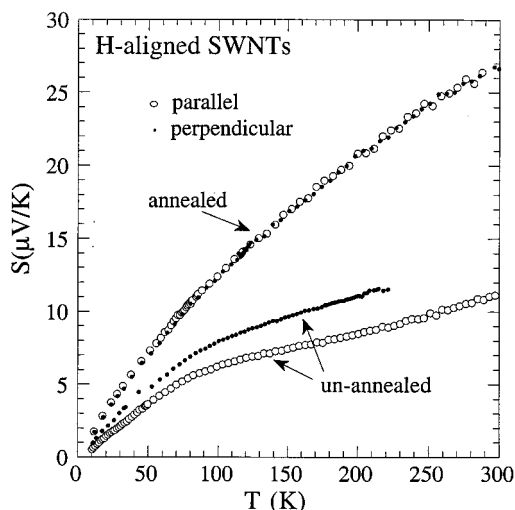


FIG. 3. Thermoelectric power of the thick aligned SWNT sample, before and after annealing. Within measurement error and sample-to-sample variations, S is independent of direction, while the magnitude of S is significantly higher after annealing.

perpendicular directions. Since the thermoelectric voltage across each element in the SWNT network is proportional to the temperature drop across it, isotropy of the TEP implies that the transverse thermal transport follows a tortuous path similar to the electronic transport. This image is also supported by the independence of $\kappa/\sigma T$ on sample morphology.

In conclusion, we have shown that the anisotropic morphology of magnetic field-aligned SWNTs leads to anisotropic electrical and thermal transport properties. Alignment of the SWNTs increases the parallel components of both the electrical and thermal conductivity with respect to unoriented material. In the parallel direction, the room-temperature electrical conductivity is of the same order as for individual SWNT ropes, and the thermal conductivity is over 200 W/mK, within an order of magnitude of that of highly crystalline diamond or graphite. The electrical and thermal conductivity change equally upon alignment, a process which is

reflected in the isotropic nature of the thermoelectric power. Further enhancements in transport anisotropies, in particular further gains in the parallel components, should be attainable by optimization of the alignment/filter deposition process.

The work at Penn supported by the National Science Foundation under the following Grants No: DMR98-02560 (J.C.H., A.T.J.), MRSEC DMR96-32598 (M.C.L., J.E.F.), and DMR97-30298 (N.M.M., J.E.F.). Work at Rice supported by NASA award No. NCC 9-77, ONR Grant No. N00014-99-1-0246, and the Welch Foundation (D.E.W., M.J.C., J.S., R.E.S.). The authors acknowledge use of the National High Magnetic Field Laboratory, which is supported by NSF Cooperative Agreement No. DMR-9527035 and the State of Florida.

- ¹D. A. Walters, M. J. Casavant, X. C. Qin, C. B. Huffman, P. J. Boul, L. M. Ericson, E. H. Haroz, M. J. O'Connell, K. Smith, D. T. Colbert, and R. E. Smalley (unpublished).
- ²B. W. Smith, Z. Benes, D. E. Luzzi, J. E. Fischer, D. A. Walters, M. J. Casavant, J. Schmidt, and R. E. Smalley, *Appl. Phys. Lett.* **77**, 663 (2000).
- ³A. G. Rinzler, J. Liu, P. Nikolaev, C. B. Huffman, F. J. Rodriguez-Macias, P. J. Boul, A. H. Lu, D. Heymann, D. T. Colbert, R. S. Lee, J. E. Fischer, A. M. Rao, P. C. Eklund, and R. E. Smalley, *Appl. Phys. A: Mater. Sci. Process.* **67**, 29 (1998).
- ⁴J. E. Fischer, H. Dai, A. Thess, R. Lee, N. M. Hanjani, D. DeHaas, and R. E. Smalley, *Phys. Rev. B* **55**, R4921 (1997).
- ⁵J. Lefebvre, M. Radosavljevic, J. Hone, and A. T. Johnson, *Phys. Rev. B* **61**, 4526 (2000).
- ⁶R. S. Lee, H. J. Kim, J. E. Fischer, J. Lefebvre, M. Radosavljević, J. Hone, and A. T. Johnson, *Phys. Rev. B* **61**, 4526 (2000).
- ⁷W. Yi, L. Lu, Z. Dian-Lin, Z. W. Pan, and S. S. Xie, *Phys. Rev. B* **59**, 9015 (1999).
- ⁸J. Hone, M. Whitney, C. Piskoti, and A. Zettl, *Phys. Rev. B* **59**, 2514 (1999).
- ⁹G. W. C. Kaye and T. H. Laby, *Tables of Physical and Chemical Constants*, 16th ed. (Longman, London, 1995).
- ¹⁰J. Hone, I. Ellwood, M. Muno, A. Mizel, M. L. Cohen, A. Zettl, A. G. Rinzler, and R. E. Smalley, *Phys. Rev. Lett.* **80**, 1042 (1998).
- ¹¹P. G. Collins, K. Bradley, M. Ishigami, and A. Zettl, *Science* **287**, 1801 (2000).
- ¹²L. Grigorian, K. A. Williams, S. Fang, G. U. Sumanasekera, A. L. Loper, E. D. Dickey, S. J. Pennycook, and P. C. Eklund, *Phys. Rev. Lett.* **80**, 5560 (1998).